Impact of Positive and Negative Lesion Site Remodeling on Clinical Outcomes

Insights From PROSPECT

Shinji Inaba, MD,*† Gary S. Mintz, MD,* Naim Z. Farhat, MD,‡ Jean Fajadet, MD,§
Dariusz Dudek, MD,‖ Antonio Marzocchi, MD,¶ Barry Templin, MBA,#
Giora Weisz, MD,*† Ke Xu, PhD,* Bernard de Bruyne, MD, PhD,**
Patrick W. Serruys, MD, PhD,†† Gregg W. Stone, MD,*† Akiko Maehara, MD*†

*New York, New York; Elyria, Ohio; Toulouse, France; Krakow, Poland; Bologna, Italy;
Santa Clara, California; Aalst, Belgium; and Rotterdam, the Netherlands*

OBJECTIVES This study investigated coronary artery remodeling patterns associated with clinical outcomes.

BACKGROUND In the prospective, multicenter PROSPECT (Providing Regional Observations to Study Predictors of Events in the Coronary Tree: An Imaging Study in Patients With Unstable Atherosclerotic Lesions) study, reported predictors of nonculprit lesion (NCL) major adverse cardiac events (MACE) were an intravascular ultrasound (IVUS) minimal lumen area (MLA) ≤ 4 mm^2, a plaque burden $\geq 70\%$, and a IVUS–virtual histology (VH) thin-cap fibroatheroma (TCFA), but not lesion site remodeling.

METHODS Overall, 697 consecutive patients with an acute coronary syndrome were enrolled and underwent 3-vessel gray-scale and IVUS-VH; 3,223 NCLs were identified by IVUS. The remodeling index (RI) was calculated as the external elastic membrane area at the MLA site divided by the average of the proximal and distal reference external elastic membrane areas. First, one third of the patients were randomly selected to determine RI cutoffs related to NCL MACE (development cohort). Receiver-operating characteristic analysis showed that there were 2 separate cut points that predicted NCL MACE: RI = 0.8789 and RI = 1.0046 (area under the curve = 0.663). These cut points were used to define negative remodeling as an RI < 0.88, intermediate remodeling as an RI of 0.88 to 1.00, and positive remodeling as an RI > 1.00. Second, we used the remaining two-thirds of patients to validate these cut points with respect to lesion morphology and clinical outcomes (validation cohort).

RESULTS Kaplan-Meier curve analysis in the validation cohort showed that NCL MACE occurred more frequent (and equally) in negative and positive remodeling lesions compared with intermediate remodeling lesions. In this cohort, negative remodeling lesions had the smallest MLA, positive remodeling lesions had the largest plaque burden, and VH TCFA, especially VH TCFA with multiple necrotic cores, was most common in negatively remodeling lesions.

CONCLUSIONS The present study showed the novel concept that positive and negative lesion site remodeling was associated with unanticipated NCL MACE in the PROSPECT study. (PROSPECT: An Imaging Study in Patients With Unstable Atherosclerotic Lesions [PROSPECT]; NCT00180466) (J Am Coll Cardiol Img 2014;7:70–8) © 2014 by the American College of Cardiology Foundation

From the *Cardiovascular Research Foundation, New York, New York; †Columbia University Medical Center, New York, New York; ‡North Ohio Heart Center/Elyria Memorial Hospital Regional Medical Center, Elyria, Ohio; §Clinique Pasteur, Toulouse, France; ‖Jagiellonian University Medical College, Krakow, Poland; ¶Policlinico Universitario S. Orsola-Malpighi, Bologna, Italy; #Abbott Vascular, Santa Clara, California; **Cardiovascular Center Aalst, OLV-Clinic, Aalst, Belgium; ††Thoraxcenter, Erasmus Medical Center, Rotterdam, the Netherlands. The PROSPECT study was funded by Abbott Vascular

Previous studies showed that a positive remodeling (lesion site external elastic membrane [EEM] area greater than the reference segments) is more common in culprit lesions in patients presenting with acute coronary syndrome and is seen in association with plaque rupture, yellow plaque color, and thrombus formation; conversely, negative remodeling (lesion EEM less than the reference segments) is more common in target lesions in patients presenting with stable symptoms (1–4). Nevertheless and surprisingly, in the prospective, multicenter PROSPECT (Providing Regional Observations to Study Predictors of Events in the Coronary Tree: An Imaging Study in Patients With Unstable Atherosclerotic Lesions) study, predictors of nonculprit lesion (NCL) major adverse cardiac events (MACE) were an intravascular ultrasound (IVUS) minimal lumen area (MLA) ≤ 4 mm^2, a plaque burden $\geq 70\%$, and a radiofrequency IVUS–virtual histology (VH) thin-cap fibroatheroma (TCFA), but not positive remodeling (5). Hibi et al. (6) showed that the frequency of positive remodeling was entirely dependent on the definition used. Therefore, we hypothesized that the lack of association between remodeling and NCL MACE in the PROSPECT study could be attributed to the approach used to assess remodeling and the definitions used to separate lesions into positive and negative remodeling.

METHODS

Protocol design. The PROSPECT study design, major inclusion and exclusion criteria, endpoints, and definitions have been described (5). In brief, 697 consecutive patients with acute coronary syndrome (ST-segment elevation myocardial infarction beyond 24 h, non–ST-segment elevation myocardial infarction, or moderate to high-risk unstable angina) were enrolled only after successful and uncomplicated percutaneous coronary intervention of all coronary lesions responsible for the index event and after completion of any other planned interventions. Three-vessel gray-scale and IVUS-VH intracoronary imaging of the left main and proximal 6 to 8 cm of each of the major epicardial coronary arteries was performed with the use of a synthetic aperture-array, 20-MHz, 3.2-French catheter (Eagle Eye, Volcano Corporation, Rancho Cordova, California) and motorized catheter pullback (0.5 mm/s). The study was approved by the institutional review board at each participating center, and all patients signed informed, written consent.

Imaging analysis. Core laboratory off-line gray-scale and IVUS-VH analyses were performed with the use of QCU-CMS software (Medis, Leiden, the Netherlands) for contouring, pcVH 2.1 software (Volcano Corporation) for contouring and data output, and proprietary qVH software (Cardiovascular Research Foundation, New York, New York) for segmental qualitative assessment and quantitative data output. All baseline IVUS images were prospectively analyzed without knowledge of subsequent events. An IVUS NCL was defined as having >3 consecutive slices with $\geq 40\%$ plaque burden.

The EEM and luminal borders were contoured for each frame. Gray-scale IVUS measurements included the cross-sectional areas (CSA) of the EEM, lumen, and plaque and media (plaque and media = EEM − lumen) and plaque burden (plaque and media ÷ EEM). Volumetric gray-scale and IVUS-VH analyses were performed using Simpson's rule. Area stenosis was calculated by the following formula: 1 − (MLA ÷ the average of the proximal and distal reference lumen CSA).

The remodeling index (RI) was calculated as the EEM CSA at the MLA site ÷ the average of the proximal and distal reference segment EEM CSAs.

Developmental and validation cohorts to determine RI cutoffs related to NCL MACE. During the process of evaluation in this entire cohort, we recognized that there might be >1 RI cutoff that was predictive of NCL MACE. Therefore, we first selected a random group of one-third of the patients enrolled in the PROSPECT study and used these

ABBREVIATIONS AND ACRONYMS

CSA = cross-sectional

DC = dense calcium

EEM = external elastic membrane

FF = fibrofatty

FT = fibrotic

IVUS = intravascular ultrasound

MLA = minimal lumen area

NCL MACE = nonculprit lesion major adverse cardiac event(s)

NC = necrotic core

RI = remodeling index

ROC = receiver-operating characteristic

TCFA = thin-cap fibroatheroma

ThCFA = thick-cap fibroatheroma

VH = virtual histology

patients to develop the cutoff values that predicted NCL MACE (development cohort). Second, we tested these remodeling cutoff values in the remaining two-thirds of patients (validation cohort) including both lesion morphology and NCL MACE.

IVUS-VH phenotype classification. IVUS-VH plaque components were color coded as dense calcium (DC, white), necrotic core (NC, red), fibrofatty (FF, light green), or fibrotic (FT, dark green). Lesions were further classified by means of IVUS-VH as one of the following: VH-TCFA, thick-cap fibroatheroma (ThCFA), pathological intimal thickening, fibrotic plaque, or fibrocalcific plaque. Fibroatheroma (both VH-TCFA and ThCFA) was defined as >10% confluent NC. VH-TCFA was a fibroatheroma without evidence of a fibrous cap with >30° of NC abutting to the lumen in at least 3 consecutive slices. ThCFA was a fibroatheroma with a definable fibrous cap. Pathological intimal thickening had a mixture of all plaque components, but dominantly FF plaque with <10% confluent NC and <10% confluent DC. Fibrotic plaque had mainly FT with <10% confluent NC, <10% confluent DC, and <15% FF plaque. Fibrocalcific plaque had mainly FT with >10% confluent DC,

but <10% confluent NC. Fibroatheromas (VH-TCFA or ThCFA) were subclassified as having single or multiple confluent NCs with or without DC.

Clinical endpoints and definitions. The pre-specified primary endpoint was the incidence of MACE, defined as the composite of death due to cardiac causes, cardiac arrest, myocardial infarction, or rehospitalization due to unstable or progressive angina according to the Braunwald Unstable Angina Classification and the Canadian Cardiovascular Society Angina Classification. The primary endpoint was adjudicated by an independent clinical events committee. On the basis of follow-up angiography, MACE was attributed to an NCL site if the site associated with an event was previously untreated. If follow-up angiography was not performed, the lesion site was classified as indeterminate and excluded from this analysis.

Statistical analysis. Statistical analysis was performed with SAS software, version 9.2 (SAS Institute, Cary, North Carolina). Categorical variables were summarized using counts and percentages. Continuous variables for baseline clinical characteristics were displayed as median and first and third interquartile range. For lesion level data, a model with a generalized estimating equation approach was used to compensate for any potential cluster effect of multiple lesions in the same patient and presented as least square means with 95% confidence intervals. Receiver-operating characteristic (ROC) cut points were selected as the points farthest away from but on a line perpendicular to the unity line to measure the ability of the RI to discriminate between the lesions with and those without NCL MACE. The ROC curves plot the probability of detecting true-positive fraction (sensitivity) against false-positive fraction (1-specificity) of 3-year NCL MACE over the entire range of the observed RI. Time-to-event data were presented as Kaplan-Meier estimates and compared with the generalized estimating equation proportional hazards model. Multivariate Cox regression models using the entire cohort were used to determine the independent predictor of NCL MACE including the previously published lesion-related variables. A p value <0.05 was considered to indicate statistical significance.

RESULTS

Patient characteristics in the entire cohort. Overall, 3,223 gray-scale IVUS lesions in 660 patients were identified. IVUS-VH data were also available for

Table 1. Baseline Clinical Characteristics of the Patients (N = 660)

Age, yrs	58.1 (50.7–66.7)
Male	77.0 (508/660)
Body mass index, kg/m^2	28.0 (25.2–31.2)
Diabetes	17.2 (113/657)
Metabolic syndrome	48.3 (308/638)
Current cigarette use	47.8 (311/651)
Hypertension	46.6 (305/654)
Hyperlipidemia	44.9 (270/601)
Previous myocardial infarction	10.7 (70/656)
Previous percutaneous coronary interventions	10.8 (71/659)
Clinical presentation	
STEMI	30.0 (198/660)
Non-STEMI	66.2 (437/660)
Unstable angina	3.8 (25/660)
Framingham Risk Score	7.0 (5.0–9.0)
Cholesterol, mg/dl	
Low-density lipoprotein	100.8 (79.2–127.4)
High-density lipoprotein	38.6 (34.0–46.0)
HbA$_{1c}$, %	5.7 (5.3–6.2)
Renal insufficiency	9.8 (61/623)
High-sensitivity C-reactive protein at 30 days, mg/dl	1.8 (0.8–4.0)

Values are median (interquartile range) or % (number of observations/total number of patients). Renal insufficiency is defined as estimated creatinine clearance ≤60 ml/min.
HbA$_{1c}$ = glycosylated hemoglobin; STEMI = ST-segment elevation myocardial infarction.
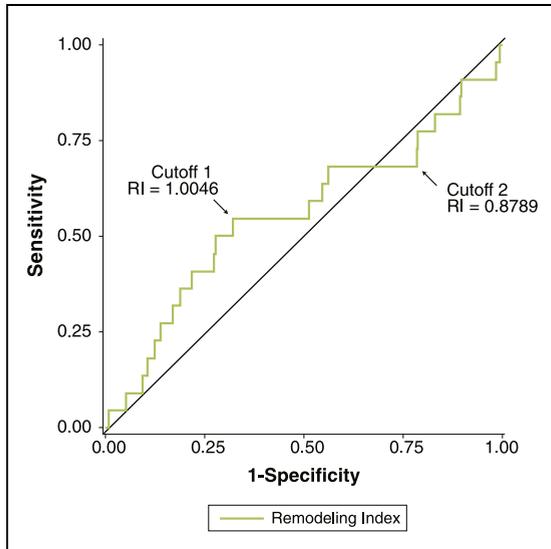
Figure 1. Receiver-Operating Characteristic Curve of RI and Nonculprit Lesion Major Adverse Cardiac Events in the Developmental Cohort

The receiver-operating characteristic curve showed 2 different cutoff values of the remodeling index (RI): 0.8789 and 1.0046.

2,874 lesions. Baseline clinical characteristics of the patients are listed in Table 1. The median age was 58.1 years, and 77.0% were men.

RI cutoffs related to NCL MACE in the developmental cohort. ROC curve analysis using a randomly selected cohort of one-third of the patients in the PROSPECT study (n = 217, 1,041 lesions) showed that there were 2 separate cutoff points (RI = 0.8789 and RI = 1.0046, area under the curve = 0.663 for this model) that predicted NCL MACE (Fig. 1). Accordingly, we divided PROS-PECT NCLs into 3 groups using these 2 cutoff points; RI <0.88 (negative remodeling), RI = 0.88 to ≤ 1.00 (intermediate remodeling), and RI >1.00 (positive remodeling).

Validation of RI cutoffs. In the remaining two-thirds of the patients in the PROSPECT study (n = 443 patients and 2,182 lesions), Kaplan-Meier curves confirmed that events occurred more frequently (and equally) in positive and negative remodeling lesions compared with intermediate remodeling lesions, as defined in the developmental cohort (p = 0.025) (Fig. 2). NCL MACE occurred in

Number at Risk							
Negative R.	734	671	657	643	629	607	391
Intermediate R.	911	841	832	807	798	775	482
Positive R.	537	488	484	460	451	435	286

Negative Remodeling (RI < 0.88)
Intermediate Remodeling (RI 0.88 – 1.00)
Positive Remodeling (RI > 1.00)
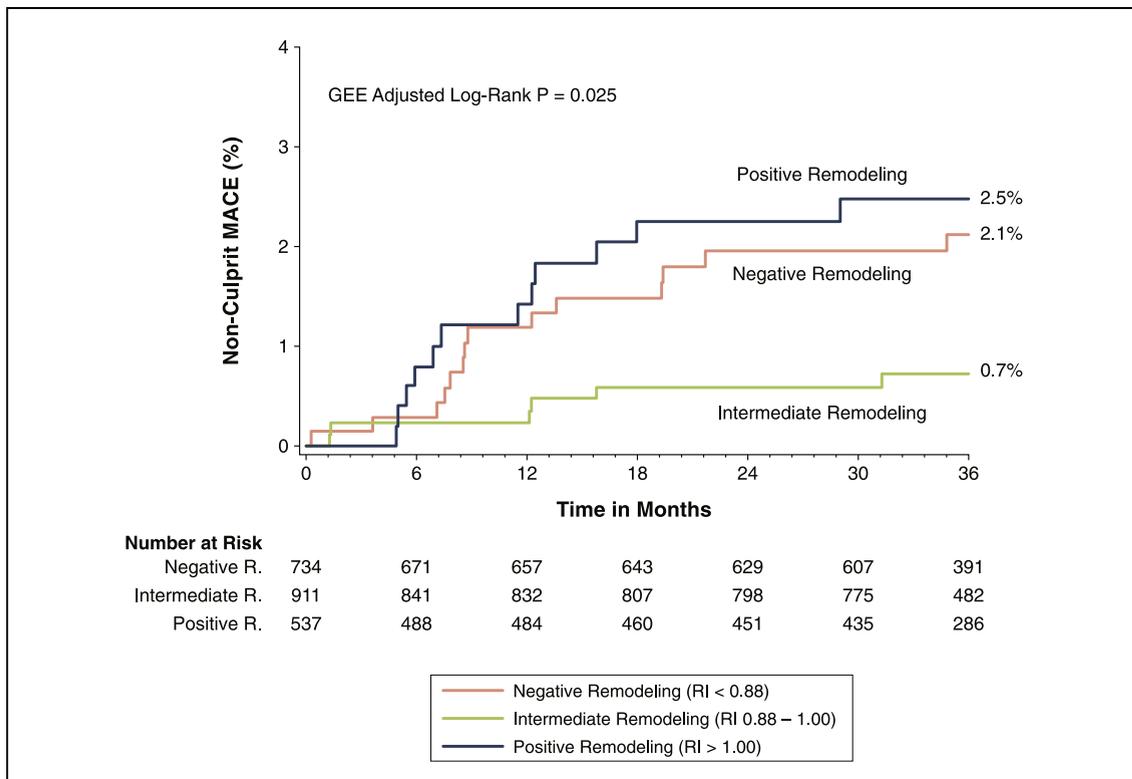
Figure 2. Kaplan-Meier Curves for MACE During 3-Year Follow-up in Nonculprit Lesions in the Validation Cohort

The 3-year cumulative rates of nonculprit lesion MACE were similarly higher in positive and negative remodeling lesions. MACE was defined as death from cardiac causes, cardiac arrest, myocardial infarction, and rehospitalization for unstable or progressive angina. GEE = generalized estimating equation; MACE = major adverse cardiac events; R = remodeling; RI = remodeling index.

Table 2. Nonculprit Lesion Events at the Lesion Level (2,182 Lesions in 443 Patients)

	RI			p Value		
	RI < 0.88 (NR, n = 734)	0.88 ≤ RI ≤ 1.00 (IR, n = 911)	1.00 < RI (PR, n = 537)	NR vs. IR	NR vs. PR	PR vs. IR
Cardiac death	0.0 (0.0)	0.0 (0.0)	0.0 (0.0)	N/A	N/A	N/A
Cardiac arrest	0.0 (0.0)	0.0 (0.0)	0.0 (0.0)	N/A	N/A	N/A
Myocardial infarction	0.1 (1.0)	0.0 (0.0)	0.0 (0.0)	<0.0001	<0.0001	N/A
Rehospitalization	2.0 (13.0)	0.7 (6.0)	2.5 (12.0)	0.03	0.49	0.008
Due to unstable angina	0.9 (6.0)	0.0 (0.0)	0.6 (3.0)	<0.0001	0.60	<0.0001
Due to progressive angina	1.0 (7.0)	0.7 (6.0)	1.9 (9.0)	0.46	0.19	0.07
Composite major adverse cardiac events	2.1 (14.0)	0.7 (6.0)	2.5 (12.0)	0.02	0.63	0.008

Events rate are shown as Kaplan-Meier estimate percentage (number of events).
IR = intermediate remodeling; N/A = not applicable; NR = negative remodeling; PR = positive remodeling; RI = remodeling index.

32 patients: 1 myocardial infarction and 31 rehospitalizations during 3 years of clinical follow-up (Table 2).

Gray-scale IVUS analysis in the validation cohort. Of the 424 patients having at least 2 NCLs, 22 patients (5.2%) had the same remodeling pattern in all lesions, whereas 402 patients (94.8%) had lesions with different remodeling patterns. The average number of NCLs per patient in the validation cohort was 4.9 ± 2.0.

As shown in Figure 3 and Table 3, the MLA was the smallest in negative remodeling lesions, with no difference between positive and intermediate remodeling lesions. On the other hand, plaque burden at the MLA site was the greatest in positive remodeling lesions, although negative remodeling lesions also had a greater plaque burden compared with intermediate remodeling lesions (Fig. 3). Negative remodeling lesions were the longest, whereas intermediate remodeling lesions were the shortest (Table 3).

IVUS-VH analysis in the validation cohort. IVUS-VH volumetric analysis showed that the percentages of NC and DC were significantly greater in negative remodeling lesions compared with the other 2 remodeling patterns (Table 4), with similar
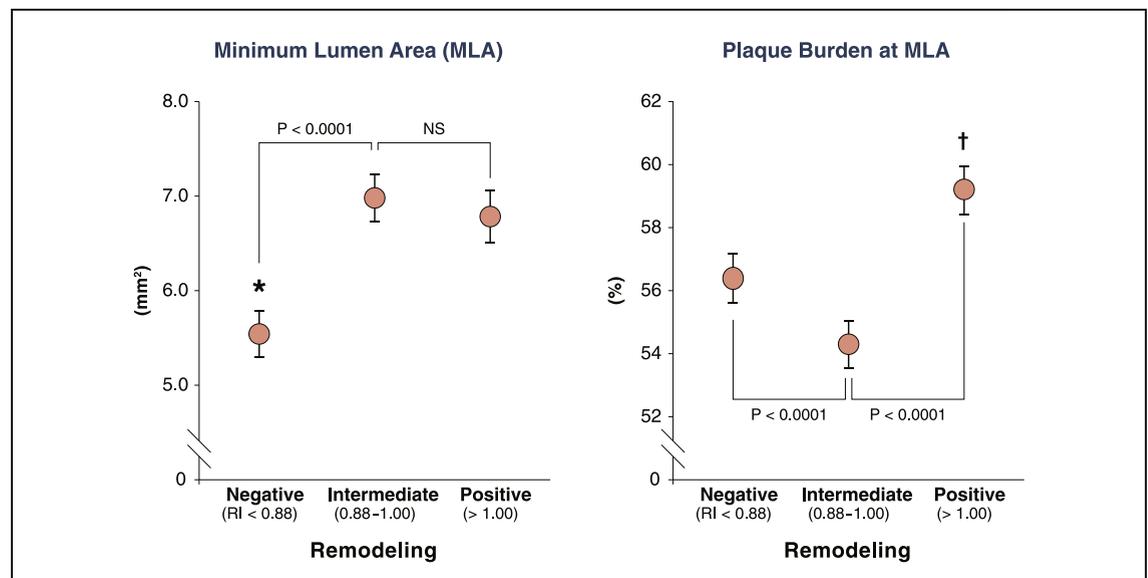
Figure 3. Difference of MLA and Plaque Burden at the MLA Site in Relation to Remodeling

(Left) The MLA; MLA is smallest in negative remodeling lesions versus positive and intermediate remodeling lesions. **(Right)** Plaque burden at the MLA site; plaque burden at the MLA site is the least in intermediate remodeling lesions compared with positive and negative remodeling lesions. The plots are displayed as least-square means with error bar (95% CI). *p < 0.0001 versus positive remodeling; †p < 0.0001 versus negative remodeling. RI = remodeling index.

Table 3. Gray-Scale Intravascular Ultrasound Lesion Analysis (2,182 Lesions in 443 Patients)

	RI			p Value		
	RI < 0.88 (NR, n = 734)	0.88 ≤ RI ≤ 1.00 (IR, n = 911)	1.00 < RI (PR, n = 537)	NR vs. IR	NR vs. PR	PR vs. IR
Minimal lumen area site						
RI	0.77 (0.76–0.78)	0.94 (0.94–0.95)	1.07 (1.06–1.07)	<0.0001	<0.0001	<0.0001
Lumen CSA, mm^2	5.5 (5.3–5.7)	7.0 (6.8–7.2)	6.8 (6.5–7.1)	<0.0001	<0.0001	0.21
Minimum lumen area ≤4 mm^2	31.1 (228)	13.8 (126)	16.6 (89)	<0.0001	<0.0001	0.16
Area stenosis, %	38.1 (37.0–39.2)	21.7 (20.7–22.7)	20.9 (19.8–22.0)	<0.0001	<0.0001	0.25
Plaque burden, %	56.5 (55.8–57.2)	54.2 (53.5–54.8)	59.2 (58.4–60.0)	<0.0001	<0.0001	<0.0001
Plaque burden ≥70%	7.4 (54)	5.2 (47)	14.2 (76)	0.10	<0.0001	<0.0001
EEM CSA at minimal lumen area, mm^2	12.8 (12.4–13.1)	15.3 (14.9–15.7)	16.7 (16.1–17.3)	<0.0001	<0.0001	<0.0001
EEM CSA at proximal reference, mm^2	19.3 (18.8–19.9)	16.8 (16.3–17.2)	16.2 (15.6–16.7)	<0.0001	<0.0001	0.04
EEM CSA at distal reference, mm^2	13.9 (13.4–14.4)	15.6 (15.2–16.1)	15.2 (14.7–15.8)	<0.0001	<0.0001	0.17
Volumetric analysis						
Lesion length, mm	21.8 (20.6–23.0)	12.5 (11.7–13.3)	13.9 (12.8–15.1)	<0.0001	<0.0001	0.04
Plaque burden, %	49.1 (48.7–49.6)	47.2 (46.8–47.7)	48.9 (48.4–49.5)	<0.0001	0.60	<0.0001
Mean EEM CSA, mm^3/mm	15.8 (15.4–16.3)	16.2 (15.7–16.6)	16.3 (15.7–16.8)	0.21	0.15	0.74
Mean lumen CSA, mm^3/mm	8.1 (7.8–8.3)	8.5 (8.3–8.8)	8.3 (8.0–8.6)	0.004	0.20	0.15
Mean plaque and media CSA, mm^3/mm	7.8 (7.5–8.0)	7.7 (7.4–7.9)	8.0 (7.7–8.3)	0.46	0.16	0.03
Morphological analysis						
Plaque rupture	3.1 (23)	2.0 (18)	3.2 (17)	0.15	0.99	0.14

Values are generalized estimating equation least-square means (95% CI) or percentage (number of observations).
CSA = cross-sectional area; EEM = external elastic membrane; other abbreviations as in Table 2.

findings for planar IVUS-VH analysis at the MLA site.

The analysis of lesion phenotype is shown in Table 4. The frequency of any fibroatheroma (combining VH-TCFA and ThCFA) was higher in negative and tended to be higher in positive remodeling lesions compared with intermediate remodeling lesions (negative remodeling vs. positive remodeling, p < 0.0001; negative remodeling vs. intermediate remodeling, p < 0.0001; intermediate remodeling vs. positive remodeling, p = 0.08). VH-TCFA was identified most frequently in negative remodeling lesions (negative remodeling vs. positive remodeling, p = 0.03; negative remodeling vs. intermediate remodeling, p = 0.003; intermediate remodeling vs. positive remodeling, p = 0.60). In addition, the frequency of VH-TCFA or ThCFA with multiple confluent NCs was more frequent in lesions with negative remodeling than positive remodeling (VH-TCFA, p = 0.01; ThCFA, p = 0.007).

Independent predictors of NCL MACE in the entire cohort. Independent predictors of NCL MACE at the lesion level are given in Table 5. In addition to previously published PROSPECT predictors of

MACE (large plaque burden, VH-TCFA, and small lumen area), both positive remodeling and negative remodeling were independent predictors of subsequent NCL MACE.

DISCUSSION

The present study suggests that the common approach of separating lesions into positive and negative remodeling or using arbitrary definitions may be too simplistic, especially when applied to NCLs. Instead, lesions at both ends of the remodeling spectrum may be most associated with future events. The present study introduced the novel concept that bidirectional remodeling was related to NCL MACE.

Determinant factors of remodeling patterns. Previous studies suggested a link between each remodeling pattern and systemic risk factors; for example, smoking and insulin-treated diabetes were associated with negative remodeling, and hyperlipidemia was associated with positive remodeling (7,8). In the present study, the majority of patients (94.8%) had different lesion-related remodeling patterns, and only a small minority had a single

Table 4. Virtual Histology Intravascular Ultrasound Lesion Analysis (1,943 Lesions in 410 Patients)

	RI			p Value		
	RI < 0.88 (NR, n = 646)	0.88 ≤ RI ≤ 1.00 (IR, n = 822)	1.00 < RI (PR, n = 475)	NR vs. IR	NR vs. PR	PR vs. IR
Minimal lumen area site, %						
Necrotic core	15.2 (14.2–16.1)	13.0 (12.1–13.8)	13.3 (12.3–14.4)	<0.0001	0.001	0.49
Dense calcium	7.7 (6.9–8.5)	5.9 (5.2–6.5)	5.6 (4.9–6.3)	<0.0001	<0.0001	0.50
Fibrous tissue	59.0 (57.9–60.0)	60.1 (59.2–61.1)	59.8 (58.7–60.9)	0.08	0.23	0.56
Fibrofatty	18.2 (17.0–19.3)	21.0 (19.9–22.1)	21.4 (20.1–22.7)	<0.0001	<0.0001	0.59
Volumetric analysis, %						
Necrotic core volume	13.8 (13.0–14.6)	12.4 (11.6–13.1)	12.6 (11.7–13.4)	0.0002	0.004	0.63
Dense calcium volume	7.2 (6.6–7.8)	6.0 (5.4–6.5)	6.2 (5.5–6.8)	<0.0001	0.003	0.58
Fibrous tissue volume	58.6 (57.8–59.4)	60.1 (59.3–60.9)	60.1 (59.1–61.0)	0.0006	0.003	0.96
Fibrofatty volume	20.5 (19.4–21.5)	21.5 (20.5–22.6)	21.2 (20.1–22.4)	0.03	0.17	0.59
Lesion phenotype						
Virtual histology derived thin-cap fibroatheroma	27.2 (176)	19.8 (163)	20.2 (96)	0.003	0.03	0.60
With multiple confluent necrotic core	20.9 (135)	13.9 (114)	14.3 (68)	0.003	0.01	0.72
With single confluent necrotic core	6.3 (41)	6.0 (49)	5.9 (28)	0.73	0.83	0.92
With dense calcium	10.1 (65)	5.7 (47)	4.4 (21)	0.007	0.002	0.41
Thick-cap fibroatheroma	44.3 (286)	33.5 (275)	37.7 (179)	<0.0001	0.03	0.15
With multiple confluent necrotic core	32.2 (208)	21.3 (175)	24.2 (115)	<0.0001	0.007	0.22
With single confluent necrotic core	12.1 (78)	12.2 (100)	13.5 (64)	0.92	0.56	0.58
With dense calcium	32.4 (209)	21.5 (177)	25.1 (119)	<0.0001	0.01	0.21
Any fibroatheroma	71.5 (462)	53.3 (438)	57.9 (275)	<0.0001	<0.0001	0.08
Pathological intimal thickening	25.1 (162)	42.5 (349)	39.6 (188)	<0.0001	<0.0001	0.33
Fibrotic plaque	2.2 (14)	3.2 (26)	2.1 (10)	0.27	0.95	0.29
Fibrocalcific plaque	1.2 (8)	1.1 (9)	0.4 (2)	0.81	0.18	0.22

Values are generalized estimating equation least-square means (95% CI) or percentage (number of observations).
  Abbreviations as in Table 2.

remodeling pattern across all lesions. This clearly indicates that remodeling is more of a lesion-specific response and less determined primarily by patient characteristics. Our data confirm the previous findings indicating heterogeneity in remodeling response, even with the same patient (9).

Positive remodeling. On the one hand, positive remodeling in response to plaque growth helps to prevent luminal narrowing (10); on the other hand, positive remodeling may be a marker for plaque vulnerability. Pathological studies revealed that plaques with positive remodeling have a larger lipid core and a greater macrophage burden typical of a rupture-prone TCFA (11,12) and consistent with previous IVUS studies in which: 1) positive remodeling is seen in patients who have a more unstable clinical presentation (4); and 2) ruptured plaque sites show more positive remodeling compared with MLA sites (13). Previous studies also

suggest that positive remodeling predicts: 1) creatine kinase-myocardial band elevation after percutaneous coronary intervention (14); 2) no reflow in primary infarct angioplasty (15); 3) recurrent ischemia within 1 month after thrombolysis for acute myocardial infarction (16); 4) target lesion revascularization in patients undergoing nonstent intervention (17); 5) MACE in patients with unstable angina undergoing any form of revascularization (18); 6) target vessel revascularization and intimal hyperplasia in patients undergoing bare metal stenting (19,20); 7) intimal hyperplasia after implantation of drug-eluting stents (21); and 8) in-hospital complications, MACE, restenosis, and new lesion formation in patients with stable angina undergoing a single-vessel intervention (22). Nevertheless, a direct relationship between positive remodeling and worse clinical outcomes has not been proved, especially in NCLs. The current study

extends previous studies and supports the concept that positive remodeling is an independent predictor of subsequent NCL MACE in PROSPECT patients.

Negative remodeling. In the present study, the mean remodeling index in the negatively remodeled lesions was 0.77, significantly lower than in previous studies (1,3,4). Moreover, in the present study, compared with positive remodeling lesions, negative remodeling lesions were longer and more calcified, consistent with advanced plaques, also similar to previous studies (9,23). Negative remodeling lesions also had the most severe stenosis. Our data were consistent with those of previous IVUS studies in which negative remodeling was a major contributor to luminal narrowing in more advanced disease (9,24). However, surprisingly, plaques with negative remodeling also had the greatest frequency of VH-TCFA, especially VH-TCFA with multiple NCs. The presence of multiple NCs was consistent with more advanced atherosclerosis in which there had been a recurring cycle of rupture and healing, as suggested by Burke et al. (25). Thus, negative remodeling was a marker of more advanced atherosclerosis to explain its ability to predict of NCL MACE (26).

Clinical events. Most events in both positive and negative remodeling lesions were rehospitalization due to unstable or progressive angina. However, the process of the development of cardiac events might have been different between negative and positive remodeling lesions. Negative remodeling physiologically contributed to symptomatic significant stenosis formation and the need for revascularization (7,9,24,26). On the other hand, positive remodeling lesions might have represented purely morphologically unstable disease. Pasterkamp et al. (27) demonstrated that local inflammation of the cap and shoulder of the plaque, promoting plaque

Table 5. Independent Predictors of Nonculprit Major Adverse Cardiac Events at the Lesion Level

	Hazard Ratio (95% Confidence Interval)	p Value
RI <0.88 vs. RI 0.88–1.00	2.39 (1.07–5.34)	0.033
RI >1.00 vs. RI 0.88–1.00	2.34 (1.00–5.44)	0.049
Plaque burden ≥70%	5.03 (2.44–10.35)	<0.0001
Virtual histology thin-cap fibroatheroma	3.05 (1.63–5.71)	0.0005
Minimum lumen area ≤4 mm^2	3.04 (1.51–6.13)	0.0018

Variables entered were RI <0.88 vs. RI 0.88–1.00, RI >1.00 vs. RI 0.88–1.00 and previously published PROSPECT predictors (plaque burden ≥70%, virtual histology thin-cap fibroatheroma, minimum lumen area ≤4 mm^2).
RI = remodeling index.

vulnerability, was more common in positive remodeling.

Study limitations. In the present study, IVUS analysis was performed at only 1 time point. Thus, these results do not reflect the dynamic interchange between remodeling and morphological behavior and its natural history. We investigated the relationship between remodeling and clinical outcomes in lesions with ≥40% plaque burden. Therefore, its relation in the early stage of atherosclerosis in vivo is still unclear.

CONCLUSIONS

Two different patterns of remodeling, not only positive remodeling, but also negative remodeling, were associated with future cardiovascular events in the PROSPECT study.

Reprint requests and correspondence: Dr. Akiko Maehara, Columbia University Medical Center/The Cardiovascular Research Foundation, 111 East 59th Street, 12th Floor, New York, New York 10022. *E-mail: amaehara@crf.org.*

REFERENCES

1. Gyongyosi M, Yang P, Hassan A, et al. Arterial remodeling of native human coronary arteries in patients with unstable angina pectoris: a prospective intravascular ultrasound study. Heart 1999;82:68–74.

2. Takano M, Mizuno K, Okamatsu K, Yokoyama S, Ohba T, Sakai S. Mechanical and structural characteristics of vulnerable plaques: analysis by coronary angioscopy and intravascular ultrasound. J Am Coll Cardiol 2001; 38:99–104.

3. Schoenhagen P, Ziada KM, Kapadia SR, Crowe TD, Nissen SE, Tuzcu EM. Extent and direction of arterial remodeling in stable versus unstable coronary syndromes: an intravascular ultrasound study. Circulation 2000;101:598–603.

4. Nakamura M, Nishikawa H, Mukai S, et al. Impact of coronary artery remodeling on clinical presentation of coronary artery disease: an intravascular ultrasound study. J Am Coll Cardiol 2001;37:63–9.

5. Stone GW, Maehara A, Lansky AJ, et al., PROSPECT Investigators. A prospective natural-history study of coronary atherosclerosis. N Engl J Med 2011;364:226–35.

6. Hibi K, Ward MR, Honda Y, et al. Impact of different definitions on the interpretation of coronary remodeling determined by intravascular ultrasound. Catheter Cardiovasc Interv 2005;65:233–9.

7. Tauth J, Pinnow E, Sullebarger JT, et al. Predictors of coronary arterial remodeling patterns in patients with

myocardial ischemia. Am J Cardiol 1997;80:1352–5.

8. Kornowski R, Mintz GS, Lansky AJ, et al. Paradoxic decreases in atherosclerotic plaque mass in insulin-treated diabetic patients. Am J Cardiol 1998; 81:1298–304.

9. Mintz GS, Kent KM, Pichard AD, Satler LF, Popma JJ, Leon MB. Contribution of inadequate arterial remodeling to the development of focal coronary artery stenoses. An intravascular ultrasound study. Circulation 1997;95:1791–8.

10. Glagov S, Weisenberg E, Zarins CK, Stankunavicius R, Kolettis GJ. Compensatory enlargement of human atherosclerotic coronary arteries. N Engl J Med 1987;316:1371–5.

11. Burke AP, Kolodgie FD, Farb A, Weber D, Virmani R. Morphological predictors of arterial remodeling in coronary atherosclerosis. Circulation 2002;105:297–303.

12. Varnava AM, Mills PG, Davies MJ. Relationship between coronary artery remodeling and plaque vulnerability. Circulation 2002;105:939–43.

13. Maehara A, Mintz GS, Bui AB, et al. Morphologic and angiographic features of coronary plaque rupture detected by intravascular ultrasound. J Am Coll Cardiol 2002;40:904–10.

14. Mehran R, Dangas G, Mintz GS, et al. Atherosclerotic plaque burden and CK-MB enzyme elevation after coronary interventions: intravascular ultrasound study of 2256 patients. Circulation 2000;101:604–10.

15. Watanabe T, Nanto S, Uematsu M, et al. Prediction of no-reflow phenomenon after successful percutaneous coronary intervention in patients with acute myocardial infarction: intravascular ultrasound findings. Circ J 2003;67:667–71.

16. Gyongyosi M, Wexberg P, Kiss K, et al. Adaptive remodeling of the infarct-related artery is associated with recurrent ischemic events after thrombolysis in acute myocardial infarction. Coron Artery Dis 2001;12: 167–72.

17. Dangas G, Mintz GS, Mehran R, et al. Preintervention arterial remodeling as an independent predictor of target-lesion revascularization after nonstent coronary intervention: an analysis of 777 lesions with intravascular ultrasound imaging. Circulation 1999;99:3149–54.

18. Gyongyosi M, Yang P, Hassan A, et al. Intravascular ultrasound predictors of major adverse cardiac events in patients with unstable angina. Clin Cardiol 2000;23:507–15.

19. Okura H, Morino Y, Oshima A, et al. Preintervention arterial remodeling affects clinical outcome following stenting: an intravascular ultrasound study. J Am Coll Cardiol 2001;37: 1031–5.

20. Endo A, Hirayama H, Yoshida O, et al. Arterial remodeling influences the development of intimal hyperplasia after stent implantation. J Am Coll Cardiol 2001;37:70–5.

21. Mintz GS, Tinana A, Hong MK, et al. Impact of preinterventional arterial remodeling on neointimal hyperplasia after implantation of (non-polymer-encapsulated) paclitaxel-coated stents: a serial volumetric intravascular ultrasound analysis from the ASian Paclitaxel-Eluting Stent Clinical Trial (ASPECT). Circulation 2003;108:1295–8.

22. Wexberg P, Gyongyosi M, Sperker W, et al. Pre-existing arterial remodeling is associated with in-hospital and late adverse cardiac events after coronary interventions in patients with stable angina pectoris. J Am Coll Cardiol 2000;36:1860–9.

23. Hassani SE, Mintz GS, Fong HS, et al. Negative remodeling and calcified plaque in octogenarians with acute myocardial infarction: an intravascular ultrasound analysis. J Am Coll Cardiol 2006;47:2413–9.

24. Pasterkamp G, Wensing PJ, Post MJ, Hillen B, Mali WP, Borst C. Paradoxical arterial wall shrinkage may contribute to luminal narrowing of human atherosclerotic femoral arteries. Circulation 1995;91:1444–9.

25. Burke AP, Kolodgie FD, Farb A, et al. Healed plaque ruptures and sudden coronary death: evidence that subclinical rupture has a role in plaque progression. Circulation 2001; 103:934–40.

26. Nishioka T, Luo H, Eigler NL, Berglund H, Kim CJ, Siegel RJ. Contribution of inadequate compensatory enlargement to development of human coronary artery stenosis: an in vivo intravascular ultrasound study. J Am Coll Cardiol 1996;27:1571–6.

27. Pasterkamp G, Schoneveld AH, van der Wal AC, et al. Relation of arterial geometry to luminal narrowing and histologic markers for plaque vulnerability: the remodeling paradox. J Am Coll Cardiol 1998;32:655–62.

Key Words: cardiovascular events ■ intravascular ultrasound ■ remodeling.